Journal of Sound and Vibration (2002) **254**(2), 219–229
doi:10.1006/jsvi.2001.3671, available online at http://www.idealibrary.com on IDEAL®

AN INVERSE AEROACOUSTIC PROBLEM ON ROTOR WAKE/STATOR INTERACTION

J. Luo and X. D. Li

Department of Jet Propulsion, No. 407, *Beijing University of Aeronautics and Astronautics, Beijing* 100083, *People's Republic of China.*
E-mails: *luojun@ns.ngl.buaa.edu.cn*; *lxd@ns.ngl.buaa.edu.cn*

(*Received* 24 *August* 2000, *and in final form* 2 *January* 2001)

An inverse aeroacoustic model on rotor wake/stator interaction is proposed based on the linearized Euler equations. The sound field is related to the pressure distribution on the stator surface in the form of a Fredholm integral equation of the first kind which is a well-known ill-posed problem. Since the sound field is fully specified, numerical inversion allows the reconstruction of the pressure distribution on the stator surface. For solving the discrete ill-posed problem, the singular-value decomposition technique coupled with the Tikhonov regularization method is applied to stabilize the solution. The optimal regularization parameter is chosen by the generalized cross-validation criterion and the discrete Picard condition is employed to analyze the ill-posedness of the inverse problem. Numerical results show that the reconstruction is fairly good when the signal-to-noise ratio is not very low. The results become inaccurate when the noise dominates over the observer signal. In addition, numerical results also indicate the importance of the reduced frequency. The higher the reduced frequency, the better the reconstruction results.

1. INTRODUCTION

Over the past few decades, the prediction and control of ducted fan noise has been one of the most important subjects in aeroacoustics. Among various kinds of sound sources of ducted fan, the rotor/stator interaction is known as one of the most important sources. Many theoretical and numerical methods have been proposed for predicting the noise generated from the rotor wake impinging on stator surfaces. Usually, most of the methods require the pressure distribution on stator surfaces either from experimental measurements or from numerical simulations. In principle, the most accurate and reliable way is to embed pressure sensors flush on the surfaces of stators. Unfortunately, it is pretty expensive as well as time consuming to carry out an experiment in terms of a very thin blade with three-dimensional (3-D) complex geometry. Therefore, it would be extremely valuable to develop some non-contact measurement techniques.

During the past few years, several inverse aeroacoustic problems have been investigated arising from various motivations. For example, Grace *et al.* [1] proposed an inversion model of gust/plate interaction based on solving the Helmholtz equation. The unsteady pressures on a zero-thickness plate were reconstructed successfully using sound field data. Very recently, this technique has been extended for a rectangular wing [2]. Yoon and Nelson [3] discussed an inversion technique aimed at active noise control of motionless sound source, detailed technical issues and some extended work can be found in reference [4]. Li [5] and Li and Zhou [6] studied the inverse problem of Ffowcs Williams–Hawkings

0022-460X/01/$35.00

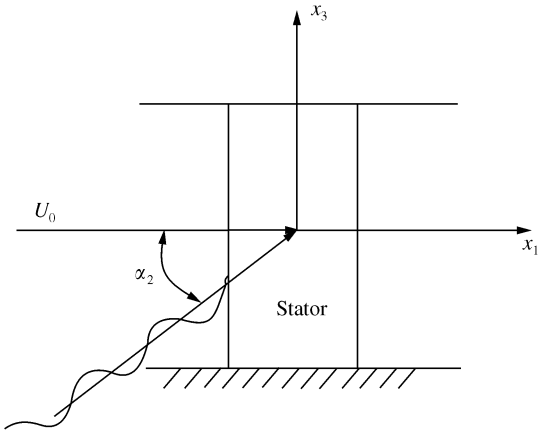

Figure 1. The co-ordinate of the cascade.

(FW–H) equation. It has been shown that the pressure distribution on an arbitrarily moving body with 3-D complex geometry could be reconstructed using finite number of acoustic data. Based on the inversion theory of the FW–H equation, a technique for spatial transformation of sound field and a new strategy for active noise control was also proposed, applicable to moving sound sources [5].

Different from previous studies, this paper proposes an inverse technique for rotor wake/stator interaction noise. The sound field is related with the unsteady pressure distributed on the stator surface in the form of a Fredholm integral equation of the first kind. Once the sound field is fully specified, numerical inversion allows the reconstruction of the pressure distribution on the stator. The main difficulty in solving the inverse problem is that it is ill-posed, which means that small errors in observer data may lead to very large solution errors unless some stability constraints are imposed. This paper will demonstrate that the Tikhonov regularization method is effective in coping with the ill-posed problem. Finally, some numerical results are presented to show the feasibility of the method.

2. BASIC FORMULATION

Assume that there is an upstream subsonic flow where the fluid is inviscid, non-heat conducting, and compressible. After making small perturbation hypothesis, the governing equations are simplified to linearized Euler equations

$$\begin{aligned} \rho_0 \frac{\mathrm{D}\mathbf{u}}{\mathrm{D}\tau} &= -\nabla\rho, \\ \frac{\mathrm{D}\rho}{\mathrm{D}\tau} &= -\rho_0 \nabla\cdot\mathbf{u}, \end{aligned} \tag{1}$$

where

$$\frac{\mathrm{D}}{\mathrm{D}\tau} = \frac{\partial}{\partial\tau} + U_0 \frac{\partial}{\partial x_1},$$

ρ_0 is the density of undisturbed medium, $\mathbf{u}$ the perturbation velocity, ρ the perturbation density, τ the time, and U_0 the mean flow velocity. The co-ordinate system is shown in Figure 1.

The above equation can be transformed into the following wave equation:

$$\frac{1}{c_0^2}\frac{\mathrm{D}^2 p}{\mathrm{D}\tau^2} - \nabla^2 p = 0, \tag{2}$$

where c_0 is the speed of sound.

Introduce the following transformation:

$$\beta = \frac{\bar{k} b \cos\alpha_2}{\beta_0^2}, \qquad \varsigma = \frac{x_1}{b}, \qquad \eta = \frac{x_2\beta_0}{b}, \qquad \xi = \frac{x_3\beta_0}{b},$$

where $\beta_0 = \sqrt{1 - M_0^2}$, b is the half-chord length of the stator blade, α_2 the angle between the propagating direction of upstream disturbance and mean flow velocity, $\bar{k}$ the incoming flow frequency, and M_0 the incoming flow Mach number (Figure 2).

The 2-D Helmholtz equation can be derived as follows:

$$\frac{\partial^2 \bar{p}}{\partial \varsigma^2} + \frac{\partial^2 \bar{p}}{\partial \eta^2} + K_\theta^2 \bar{p} = 0, \tag{3}$$

where

$$k_\theta = \frac{\bar{k} b}{\beta_0^2}\sqrt{(M_0^2 - \sin^2\alpha_2)},$$

$$\bar{p}(\varsigma, \eta) = p \exp\left\{ \mathrm{i}\left[\beta M_0^2 x_1 + \bar{k} U_0 \tau - \frac{\bar{k} b \sin\alpha_2}{\beta_0} x_3 \right]\right\}.$$

Following Sun *et al.* [7] (the only difference is that here we neglect the effect of swept angle), the radiated sound field can be expressed in the following form:

$$p^{\pm} = \sum_{n=m_1}^{m_2} p_n^{\pm}, \tag{4}$$

where

$$p_n^{\pm} = A_n f_0(K_\theta \sin\Theta_n^{\pm}), \tag{5}$$

$$A_n = \frac{b}{2k_n d}\left(\frac{\sigma - 2n\pi}{d}\cos\theta - \gamma_n \sin\theta\right) \times \exp \mathrm{i}\left[-\bar{k} U_0 \cos\alpha_2 \tau + \frac{\sigma - 2n\pi}{d} y_2 + \gamma_n y_1 + \bar{k}\sin\alpha_2 y_3 \right],$$

$$k_n = \sqrt{k_0^2 - \beta_0^2\left[\left(\frac{\sigma - 2n\pi}{d}\right)^2 + (\bar{k} M_0 \sin\alpha_2)^2\right]},$$

$$k_0 = \frac{M_0 \sin\theta(\sigma - 2n\pi)}{d} - \bar{k} M_0,$$

$$\gamma_n = \frac{1}{\beta_0^2}[M_0 k_0 \pm k_n],$$

$$y_1 = b\varsigma\cos\theta - b\eta\sin\theta, \qquad y_2 = b\varsigma\sin\theta + b\eta\cos\theta, \qquad y_3 = x_3,$$

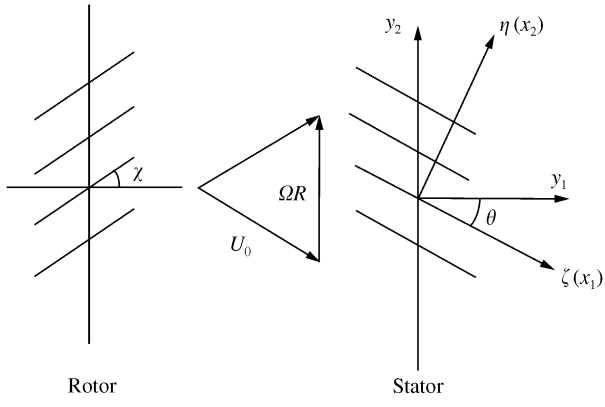

Figure 2. Rotor and stator.

$$f_0(K_\theta \sin \Theta_n^{\pm}) = \int_{-1}^{1} \Delta p(\varsigma) \exp[-\mathrm{i}(K_\theta \sin \Theta_n^{\pm} - K_r M_0)\varsigma] \, \mathrm{d}\varsigma,$$

$$K_r = \frac{\bar{k} b M_0 \cos \alpha_2}{\beta_0^2}.$$

In the above formulas, θ and χ are the stagger angle of stator and rotor, respectively, $f_0(K_\theta \sin \Theta_n^{\pm})$ the Fourier transformation result of the unsteady pressure difference between upper and lower surfaces, d the blade spacing of stator, σ the interblade phase angle (the phase difference of upwash velocity between neighbouring blades), $p^{\pm}$ the sound pressure, $p_n^{\pm}$ the sound pressure of each acoustic mode, the subscripts " + " and " − " stand for the sound waves travelling downstream and upstream, respectively, and m_1 and m_2 are the wave numbers that satisfy the cut-on condition [8]. Δp denotes the unsteady pressure difference between the upper and lower stator surfaces.

As for rotor wake/stator interaction, since every rotor blade sheds a wake, the flow field due to all wakes is the superposition of infinite rotor blade wakes, which can be expanded as Fourier series [9]:

$$u_2 = \sum_{n=-\infty}^{+\infty} W_q \sin(\theta + \chi) \exp\left\{\mathrm{i}\left[\bar{k}\zeta + n\frac{2\pi q B}{V} - qB\Omega\tau\right]\right\}, \tag{6}$$

where

$$W_q = W_c \sqrt{\frac{\pi}{\delta}} \frac{2l}{d_r \cos \chi} \exp\left[\left(\frac{\pi q l}{d_r \cos \chi}\right)^2 \Big/ \delta\right].$$

In the above formula, W_c is the maximum wake perturbation velocity, d_r the rotor blade spacing, l the wake halfwidth, and δ is a parameter that can be adjusted for optimum data fit [9]. B and V are the number of rotor blade and stator blade, respectively, and q the harmonic number. For such kind of disturbing waves, the interblade phase angle $\sigma = 2\pi q B/V$.

Dividing the chord into N elements, the discrete form of equation (5) is

$$p_n^{\pm} = A_n \times \sum_j \Delta p(j) \mathrm{e}^{-\mathrm{i}(K_\theta \sin \Theta_n^{\pm} \zeta_j - K_r M_0)} \delta l_j. \tag{7}$$

The exponent is associated with changes in retarded time [8].

3. ANALYSIS AND SOLUTION OF INVERSE PROBLEMS

For the analysis and solution of the inverse problem described above, equation (7) is further written in an abstract form as

$$Ax = b, \tag{8}$$

where A is the model matrix with an overdetermined dimension with $m \geqslant n$, x corresponds to the unsteady pressure on the stator surface, and b stands for the sound pressure of finite number of observing points.

Following the work of Li [5] and Li and Zhou [6], we use Tikhonov regularization [10] coupled with singular-value decomposition [11]. The essence of this approach is to find the minimum norm solution of the following least-squares problem:

$$\min_x \{ \|Ax - b\|_2 + \lambda \|Lx\|_2 \}, \tag{9}$$

where λ controls the weight given to a minimization of the seminorm $\|Lx\|_2$ of the solution relative to minimization of the residual norm $\|Ax - b\|_2$.

Singular-value decomposition (SVD) is a widely used technique for decomposing an ill-conditioned matrix which can be represented in the following form:

$$A = U\Sigma V = \sum_{i=1}^{n} u_i \sigma_i v_i^{\mathrm{T}}, \tag{10}$$

where $U = (u_1, \ldots, u_n)$ and $V = (v_1, \ldots, v_n)$ are matrices with orthonormal columns, $U^{\mathrm{T}}U = I_m$, $V^{\mathrm{T}}V = I_n$, and T denotes transposition. Σ is an $m \times n$ diagonal matrix which contains the singular values in descending order of magnitude progressing down the diagonal, i.e.,

$$\sigma_1 \geqslant \cdots \geqslant \sigma_n \geqslant 0. \tag{11}$$

For Tikhonov regularization, $L = I_n$, the solution of equation (8) can be expressed as

$$x_{reg} = \sum_{i=1}^{n} \sigma_i \frac{u_i^{\mathrm{T}} b}{\sigma_i^2 + \lambda^2} v_i. \tag{12}$$

It is very clear to see from equation (12) how the parameter λ can deviate the singularities: even if σ_i decays to zero, division by zero does not occur. For an ill-conditioning matrix A, a cluster of singular values are very close to zero, some of them are dominated by the round-off errors of the computer, they will make the solution oscillate. The function of the regularization parameter λ is to filter out the influence of these components, thus making the solution stable.

There is an underlying assumption of using the Tikhonov regularization method which states that the errors on the right-hand side are unbiased and their covariance matrix is proportional to the identity matrix. Furthermore, no matter which kind of regularization method is used, it must satisfy the discrete Picard condition (DPC) [12] which states that the Fourier coefficients $|u_i^{\mathrm{T}} \bar{b}|$ decay to zero faster than the generalized singular value γ_i. For Tikhonov regularization, $L = \mathrm{I}_n$ and $\gamma_i = \sigma_i$. The DPC plays an important role in the analysis of the discrete ill-posed problems. When the DPC cannot be satisfied, the reconstruction results will deviate from the exact solution a lot even if regularization methods have been utilized.

In the above Tikhonov regularization method, the choice of the regularization parameter λ is undoubtedly of great importance. A suitable regularization parameter can appropriately filter out the influence of perturbed errors, thus making the solution stable and reasonable. In this paper, we employ the generalized cross-validation (GCV) criterion [13] to choose the regularization parameter. The basic formula of GCV can be expressed as

$$V(\lambda) = \frac{\|(I - P(\lambda)\|^2}{[trace(I - P(\lambda))]^2}, \tag{13}$$

in the case of Tikhonov regularization,

$$P(\lambda) = A(A^{\mathrm{T}}A + \lambda^2 I)^{-1} A^{\mathrm{T}}, \tag{14}$$

using $z = U^{\mathrm{T}}b$, equation (13) can be written as

$$V(\lambda) = \frac{\|b\|^2 - \|z\|^2 + \sum_{i=1}^{n} [\lambda^2/(\sigma_i^2 + \lambda^2)]^2 z_i^2}{[m - n + \sum_{i=1}^{n} \lambda^2/(\sigma_i^2 + \lambda^2)]^2}. \tag{15}$$

The optimal value of regularization parameter λ_{opt} is determined by minimization of $V(\lambda)$ once the SVD of $P(\lambda)$ has been completed equation (15) indicates that for most cases, $\sigma_n \leqslant \lambda_{opt} \leqslant \sigma_1$. Bringing λ_{opt} into equation (12), the optimal regularization solution x_{reg} can be obtained.

4. RESULTS AND DISCUSSION

To demonstrate the feasibility of the method proposed above, several numerical examples are presented. The main parameters of blades are: rotor blade number is 14, stator blade number is 18, rotating speed of the rotor is 917·56 rad/s, spacing to chord ratio of stator is 3·8, stagger angles of rotor and stator are $\pi/6$ and 0 respectively. The observer numbers are 10 and 7 in the upstream and downstream respectively. The grid points number on the stator surface is 30.

The following procedure is used in numerical tests:

(1) Calculate the unsteady pressure distribution on blades based on the work of Sun *et al.* [7].
(2) The sound field is predicted by equation (4).
(3) The blade surface unsteady pressure distribution is reconstructed using equation (12).

Since the sound energy of rotor wake/stator interaction noise is mainly distributed on the blade passing frequency (BPF) and its second harmonic (2BPF), we focus our work on the inversion of the first and second harmonics of BPF of the unsteady pressures.

To simulate the measurement errors as in real physical cases, random errors are added to exact sound signals as

$$[p]_m = [p]_d + e, \tag{16}$$

where $[p]_m$ is the simulated sound pressure, $[p]_d$ the exact sound pressure which is obtained from equation (4), and e the perturbation vector which has zero mean and covariance matrix $\sigma_g^2 = I_m$. The signal-to-noise ratio is defined as follows:

$$\frac{S}{N} = \left[\frac{1}{m}\frac{\|[p]_d\|^2}{\sigma_g^2}\right]^{1/2}. \tag{17}$$

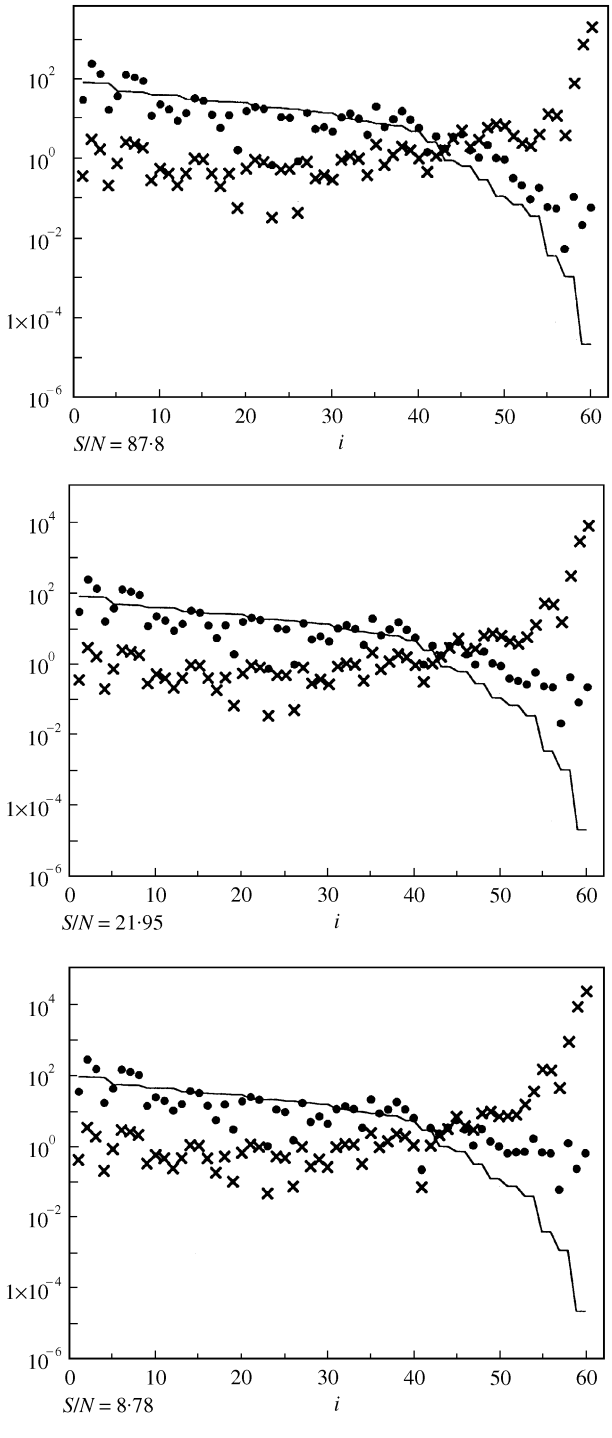

Figure 3. The discrete Picard conditions: ——, σ_i; ●, $u_i^{\mathrm{T}} b$; **x**, $u_i^{\mathrm{T}} b/\sigma_i$.

For the case of blade passing frequency (BPF), first of all, we analyze how well the DPC is satisfied for different S/N as shown in Figure 3. In this tests case, for large signal-to-noise ratio ($S/N = 87{\cdot}8$), the Fourier coefficients decay to zero faster than the singular values in

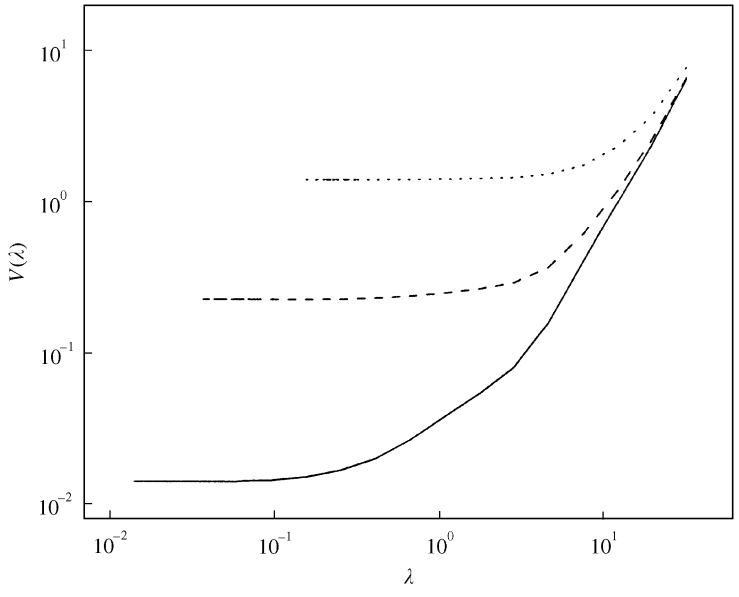

Figure 4. Generalized cross-validation functions: ——, $S/N = 87{\cdot}8$; $\lambda = 2{\cdot}76\text{E} - 2$; - - - -, $S/N = 21{\cdot}95$; $\lambda = 7{\cdot}73E - 2$; · · · ·, $S/N = 8{\cdot}78$; $\lambda = 2{\cdot}33E - 1$.

the left part of the singular values curve (for $i \leqslant 53$). This means the DPC has been satisfied rather well which renders the regularization parameter λ_{opt} chosen by GCV criterion capable of removing the perturbation and round-off errors effectively. A basic principle is that the regularization parameter λ_{opt} increases with signal-to-noise ratio decreasing, see Figure 4. From this it is easy to understand that a stable solution can be obtained only when the perturbation components have been filtered out completely. Figure 5(a–f) shows the reconstruction results for the blade passing frequency component of the unsteady pressure. In order to include the effects of the higher order evanescent-like waves, the total number of acoustic modes included in the calculation was 101 ($n = \pm 50$). The results indeed agree fairly well with the exact solution for large S/N. With S/N decreasing, the Fourier components satisfying the DPC are also decreasing, thus the satisfaction condition of discrete Picard condition is becoming worse. For $S/N = 21{\cdot}95$, the number of Fourier coefficients of the model matrix that decay to zero faster than singular values is smaller than before ($i \leqslant 42$); this means the DPC cannot be satisfied well which results in a deviation between the reconstruction and the exact solution. For $S/N = 8{\cdot}78$, the satisfaction condition of DPC is becoming even worse, large errors are expected to occur in the reconstruction results. For low signal-to-noise ratio, since the regularization parameter cannot effectively remove the perturbation errors, some numerical oscillations occur in the reconstruction especially in the leading edge and trailing edge.

Figure 6(a–f) gives the reconstruction results for 2BPF. A remarkable phenomenon is that the inversion results are much better under the same signal-to-noise ratio. This is because with frequency increasing, more acoustic modes can satisfy the cut-on condition [7] and propagate to the far field so that the sound pressure obtained from observers will contain more information about the sound source. This can also be explained as follows: for lower frequency, the exponent term in equation (7) which is associated with the changes in retarded time will show small variation when the source point co-ordinate ζ on the cascade varies from -1 to 1. This means the far field does not depend on the details of the unsteady

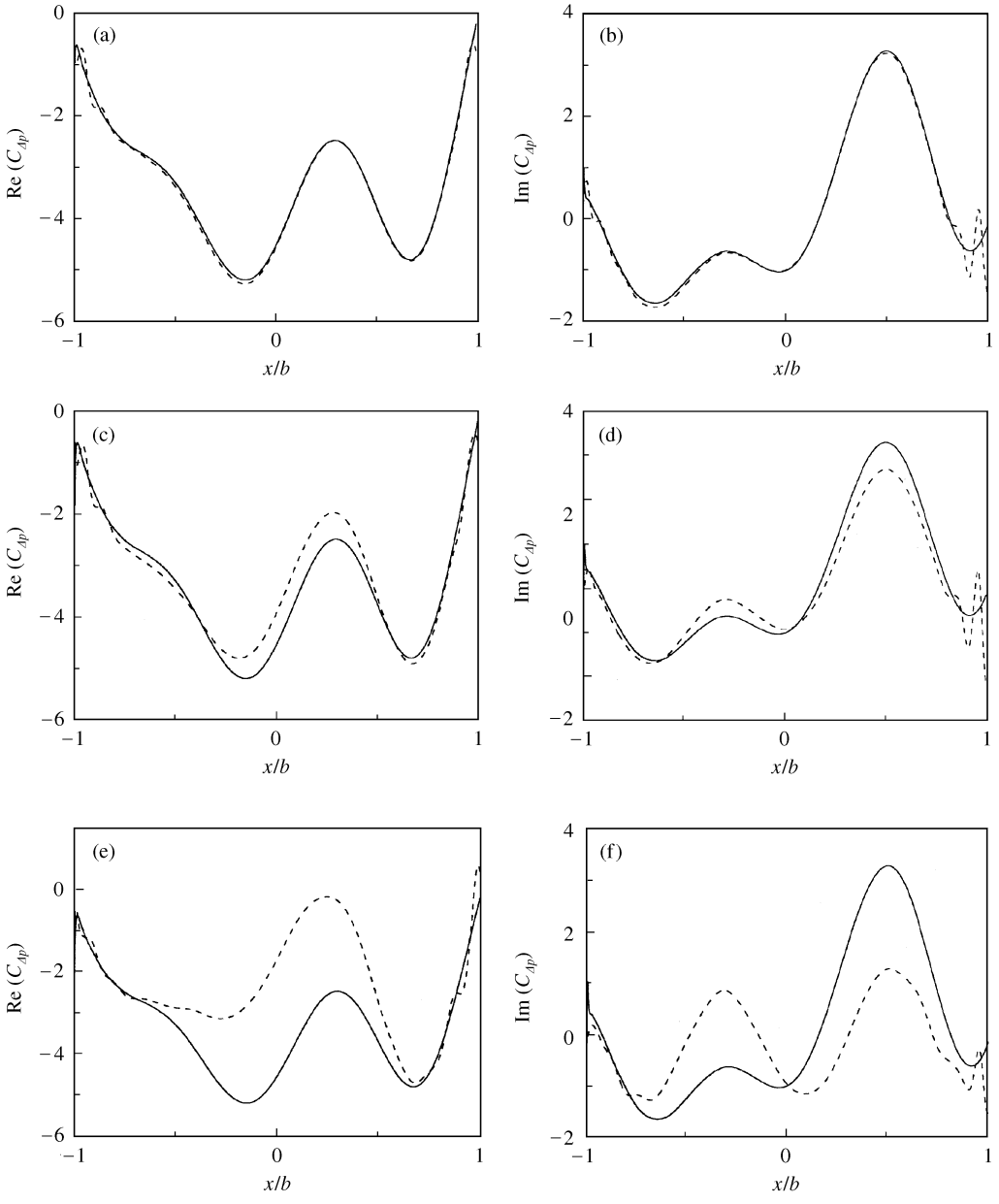

Figure 5. Comparison of reconstructions under different S/N for BPF: (a, b) ——, exact solution; - - - - -, $S/N = 87{\cdot}8$; (c, d) ——, exact solution; - - - - - -, $S/N = 21{\cdot}95$; (e, f) ——, exact solution; - - - - - -, $S/N = 8{\cdot}78$.

pressure on the stator surface so that the sound pressure information obtained from observers is not enough to discern the details of the sound source. A similar phenomenon has been observed by Patrick *et al.* [14] whose work is focused on the inverse aeroacoustic problem on gust/plate interaction.

From the numerical results, we can see that the reconstruction results are rather good when signal-to-noise ratio is not very low. However, the results are still dissatisfactory for lower signal-to-noise ratio which remains a challenging task worthy of further research.

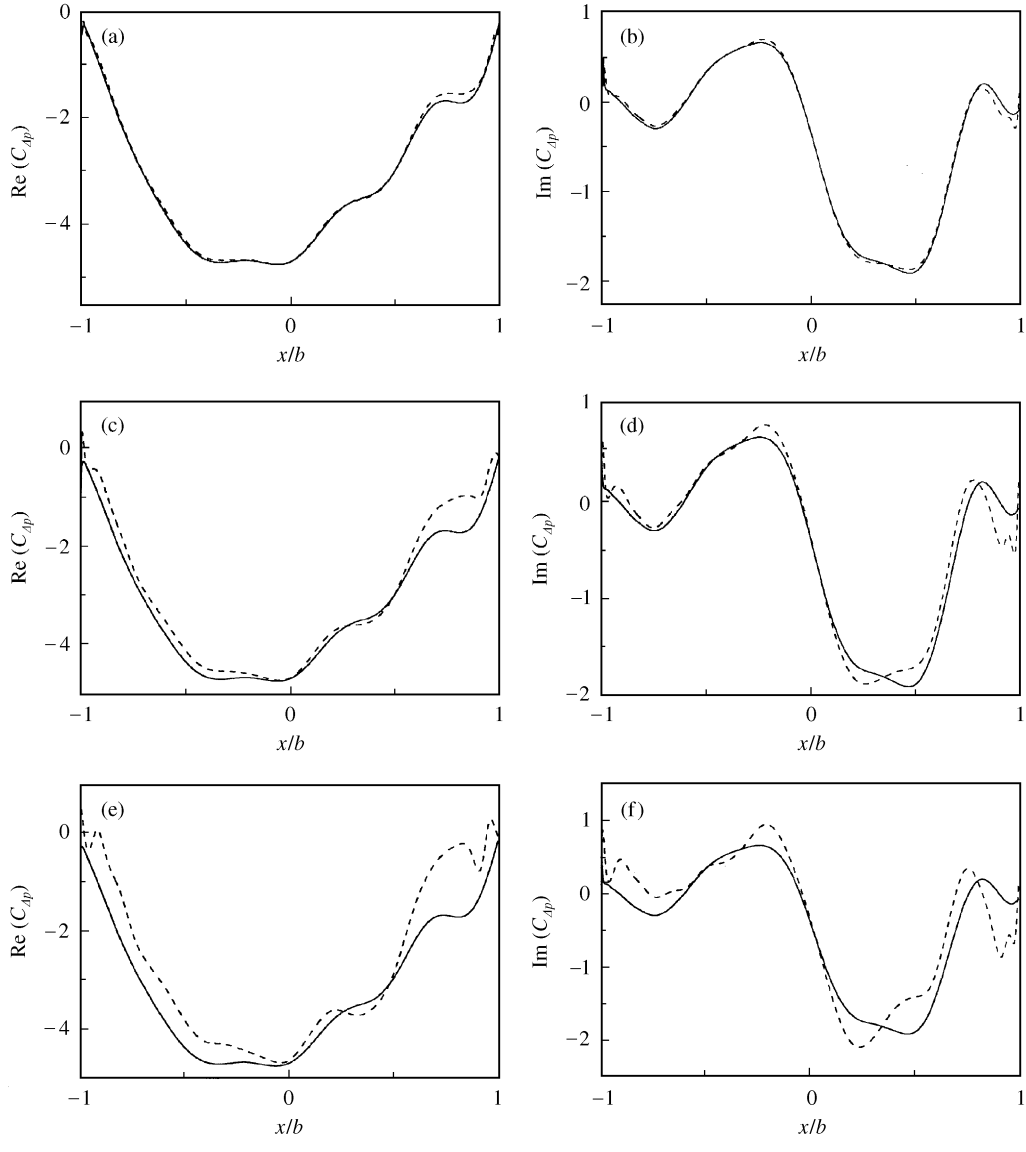

Figure 6. Comparison of reconstructions under different S/N for 2BPF: (a, b) ——, exact solution; - - - - -, $S/N = 87{\cdot}7$; (c, d) ——, exact solution; - - - - -, $S/N = 21{\cdot}87$; (e, f) ——, exact solution; - - - - -, $S/N = 8{\cdot}77$.

5. CONCLUDING REMARKS

An inverse aeroacoustic model on rotor wake/stator interaction is proposed in this paper. Based on the linearized Euler equations, the unsteady pressure distribution on the stator surface is related with the sound field of a finite number of observers in the form of a Fredholm integral equation of the first kind. Once the sound field is known, the unsteady pressure on the stator surface can be obtained by numerical inversion. Computation results demonstrate the feasibility of the inversion model and the reconstruction method.

The main difficulty in solving the inverse problem is its ill-posedness. To overcome this difficulty, the Tikhonov regularization method combined with singular-valve

decomposition is employed to stabilize the solution. The main idea of this method is to filter out the influence of perturbation errors that are mainly dominated by the round-off errors of the computer, thus making the solution stable. An investigation of how heavy the ill-posed inverse problems are is discussed using the discrete Picard condition. Numerical results show that the reconstruction accuracy depends to a great extent on how well the discrete Picard condition can be satisfied.

Numerical results show that the reconstruction results are accurate enough when the signal-to-noise ratio is not very low. The reconstruction results become inaccurate when the perturbation errors dominate over the observer data. In addition, the comparison of reconstruction results of BPF and 2BPF of unsteady pressure shows that the reduced frequency has a great effect on the reconstruction results.

ACKNOWLEDGMENT

This work is sponsored by National Natural Science Foundation of China (NSFC-59606003) and National Aeronautical Science Foundation of China (ASFC-97C51102). The authors are grateful to Prof. Xiaofeng Sun for his continuous assistance and fruitful discussions.

REFERENCES

1. S. P. GRACE and H. M. ATASSI 1996 *American Institute of Aeronautics and Astronautics Journal* **34**, 2233–2240. Inverse aeroacoustic problem for a streamlined body, Part 1: basic formulation.
2. T. H. WOOD and S. M. GRACE 2000 *American Institute of Aeronautics and Astronautics Journal* **38**, 203–210. Inverse aeroacoustic problem for a rectangular wing.
3. S. H. YOON and P. A. NELSON 1998 *AIAA*-98-2339. Reconstruction of aeroacoustic source strength distributions by inverse techniques.
4. S. H. YOON and P. A. NELSON 2000 *Journal of Sound and Vibration* **233**, 634–705. Estimation of acoustic source strength by inverse methods.
5. X. D. LI 1995 *Ph.D. Dissertation, Department of Jet Propulsion, Beijing University of Aeronautics and Astronautics, Beijing, People's Republic of China., May*. A new kind of inverse problem in aerodynamics and aeroacoustics.
6. X. D. LI and S. ZHOU 1996 *American Institute of Aeronautics and Astronautics Journal* **34**, 1097–1102. Spatial transformation of discrete sound field from a propeller.
7. X. F. SUN, Z. A. HU and S. ZHOU 1990 *AIAA* 90-3988. Theoretical investigation of noise generated by swept cascade.
8. M. E. GOLDSTEIN 1976 *Aeroacoustics*. New York: McGraw-Hill International Book Company.
9. E. ENVIA and E. J. KERSCHEN 1984 *AIAA*-84-2326. Noise produced by the interaction of rotor wake with a swept stator blade.
10. A. N. TIKHONOV 1963 *Doklady Akademiya Nauk SSSR* **151**, 501–504 (*Soviet Mathematics Doklady* **4**, 1035–1038. Solution of incorrectly formulated problems and the regularization method.
11. G. H. GOLUB and W. KAHAN 1965 *SIAM Journal on Numerical Analysis* **2**, 205–224. Calculating the singular value decomposition and pseudo-inverse of a matrix.
12. P. C. HANSEN 1990 *Bit* **30**, 658–672. The discrete Picard condition for discrete ill-posed problems.
13. G. H. GOLUB, M. HEATH and G. WAHBA 1979 *Technometrics* **21**, 215–223. Generalized cross-validation as a method for choosing a good ridge parameter.
14. S. M. PATRICK and H. M. ATASSI 1995 *CEAS/AIAA*-95-162. Predicting the unsteady pressure on a streamlined body from its acoustic signal.